Transfer Learning-Based Design Method for Cogging Torque Reduction in PMSM With Step-Skew Considering 3-D Leakage Flux

Yun-Jae Won[1], Jae-Hyun Kim[2], Soo-Hwan Park[2], Ji-Hyeon Lee[1], Soo-Min An[1], Doo-Young Kim[3], and Myung-Seop Lim[2]

[1]Department of Automotive Engineering (Automotive-Computer Convergence), Hanyang University, Seoul 04763, Republic of Korea
[2]Department of Automotive Engineering, Hanyang University, Seoul 04763, Republic of Korea
[3]C-MDPS Parts Engineering Cell, Hyundai Mobis, Yongin 16891, Republic of Korea

Step-skew is a common technique for eliminating the cogging torque of a target harmonic order in permanent magnet synchronous motors (PMSMs). However, when step-skew is applied to the rotor, the cogging torque of the target harmonic order is not completely eliminated due to 3-D leakage flux. Therefore, the 3-D leakage flux should be considered in designing a PMSM with step-skew for cogging torque reduction. The most accurate way to consider the 3-D leakage flux is to perform 3-D finite element analysis (FEA), but it has the disadvantage of high computation time. To resolve this challenge, this article proposes a design method that utilizes transfer learning to reduce the time for 3-D FEA while maintaining accuracy. Through the proposed method, a large amount of 2-D FEA-based data and a small amount of 3-D FEA-based data are used instead of a large amount of 3-D FEA-based data, with similar accuracy as using a large amount of 3-D FEA-based data, and the computational time is highly reduced. Finally, a prototype is fabricated and tested to verify the validity of the proposed design method for cogging torque reduction.

***Index Terms*— 3-D leakage flux, cogging torque, deep neural network (DNN), permanent magnet synchronous motors (PMSMs), step-skew, transfer learning.**

I. Introduction

COGGING torque is a type of reluctance torque, which is caused by the interaction between the magnetomotive force of the permanent magnet (PM) and the variable reluctance of the slotted stator as the PM rotates past the slot openings [1]. The cogging torque is the primary source for the torque ripple of PM synchronous motors (PMSMs), which leads to mechanical vibration and acoustic noise. Reducing cogging torque is essential for applications requiring high precision and smooth operation of PMSMs, such as conveyor systems, pumps, and fans. Many techniques for reducing cogging torque in PMSMs have been broadly investigated, such as applying skew angle to poles and slots [2], selecting the combination of the number of slots and poles [3], shifting of the PMs [4], optimizing the magnet pole-arc width [5], stator teeth pairing design [6], teeth notching [7], and so on.

The cogging torque occurs with a period of the least common multiple of the number of poles and slots. Ideally, this cogging torque of fundamental wave order can be completely eliminated by applying an optimal skew angle. However, this optimal skew angle is based on the ideal assumption that the PMSM has an infinite stack length and no axial leakage flux. Accordingly, the cogging torque of the target harmonic order still exists at the conventional theoretical optimal skew angle due to the 3-D leakage flux in PMSMs with step-skew. Especially, it is more apparent at shorter stack length. However, since 3-D finite element analysis (FEA) should be performed to consider the 3-D leakage flux, high computation time is required.

Therefore, this article proposes a computationally efficient design method while considering 3-D leakage flux to reduce cogging torque in PMSM with step-skew. First, the similar tendency between the 3-D FEA-based cogging torque of a target harmonic order in PMSMs with step-skew and 2-D FEA-based cogging torque of the target harmonic order in PMSMs without step-skew was presented and verified using FEA. Then, a transfer learning-based surrogate model was built to reduce computation time in the cogging torque reduction design stage. For this transfer learning, a large amount of 2-D FEA data and a small amount of 3-D FEA data were used. To validate the effectiveness of the proposed method, two PMSMs were optimized: conventional method and proposed method, and their cogging torque was compared using 3-D FEA. Finally, a prototype of an optimized PMSM with the proposed method was fabricated and verified through test.

II. 3-D Effects and Cogging Torque Tendency

In this section, the effect of axial leakage flux on cogging torque was verified using 2-D FEA and 3-D FEA, and the tendency of 2-D FEA-based cogging torque without step-skew and 3-D FEA-based cogging torque with step-skew according to the geometry variables was analyzed. The analysis was performed with the target model of the surface-mounted PMSM (SPMSM). The specifications and geometry of the target model are summarized in Table I and Fig. 1.

Manuscript received 28 March 2023; revised 3 July 2023; accepted 5 July 2023. Date of publication 17 July 2023; date of current version 24 October 2023. Corresponding author: M.-S. Lim (e-mail: myungseop@hanyang.ac.kr).

Color versions of one or more figures in this article are available at https://doi.org/10.1109/TMAG.2023.3294601.

Digital Object Identifier 10.1109/TMAG.2023.3294601

0018-9464 © 2023 IEEE. Personal use is permitted, but republication/redistribution requires IEEE permission.
See https://www.ieee.org/publications/rights/index.html for more information.

Authorized licensed use limited to: Hanyang University. Downloaded on October 25,2023 at 00:35:08 UTC from IEEE Xplore. Restrictions apply.

TABLE I
TARGET MODEL SPECIFICATIONS

Parameters	Values	Unit
Number of poles / slots	8 / 12	-
DC link voltage	12.0	V_{dc}
Current limit	40.0	A_{rms}
Current density	15.0	A_{rms}/mm^2
Slot fill factor	45.0	%
PM residual magnetic flux density	1.39	T(@20°C)
Stator outer diameter	86.0	mm
Air gap length	1.0	mm
Stack length	18.0	mm
Rated speed	1000	rpm
Rated torque	2.1	Nm

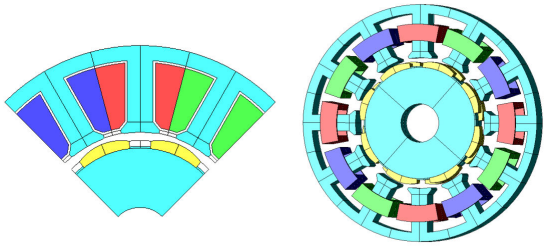

(a) (b)

Fig. 1. Geometry of the target model. (a) 2-D FEA. (b) 3-D FEA.

A. Effect of 3-D Leakage Flux on Cogging Torque

The cogging torque of PMSMs can be expressed in the general form [3]:

$$T_{\text{cog}} = \sum_{i=1,2,3,\ldots}^{\infty} K_{\text{sk}} T_i \sin(i N_c \theta) \tag{1}$$

where N_c is the fundamental order, which is the least common multiple between the number of rotor poles and the number of stator slots, θ is the mechanical angle between the stator and rotor, and K_{sk} is the skew factor. The cogging torque has a periodicity equal to the least common multiple between the number of poles and slots per mechanical period. Through this periodicity and the number of rotor steps, the theoretical skew angle to eliminate the cogging torque of the fundamental wave order can be calculated. For a step-skewed rotor, the theoretical skew angle between the first and last steps of the rotor can be calculated as follows:

$$\theta_{\text{skew}} = \frac{360^\circ}{N_c} \times \frac{n-1}{n} \tag{2}$$

where n is the number of rotor steps. For 8-poles 12-slots SPMSM, a 24th cogging torque of the mechanical rotation speed is generated, and the skew angle of the two rotor steps to eliminate the cogging torque of the target harmonic is 7.5°. However, when the 3-D FEA was performed under no-load condition applying the skew angle (7.5°), magnetic flux in the Z-axis direction is generated at the junction and both ends of the PMs, as shown in Fig. 2, so the 24th cogging torque is not completely eliminated. This axial leakage flux does not contribute to the output torque and can significantly affect the cogging torque of the PMSMs, especially in PMSMs with short stack length or a high number of pole pairs. This is because the axial leakage flux interacts with the main air-gap magnetic flux to increase the cogging torque.

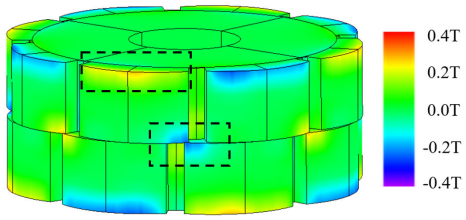

Fig. 2. Magnetic flux density contour in the Z-axis direction.

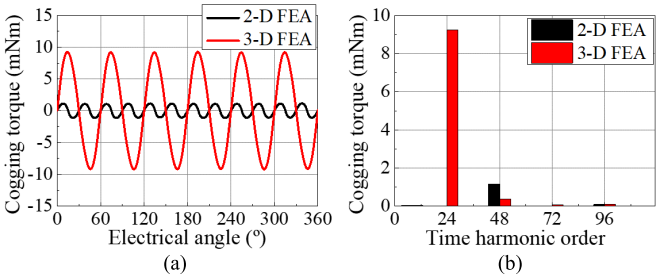

Fig. 3. Comparison of 2-D and 3-D FEA-based cogging torque of SPMSM with step-skew. (a) Cogging torque waveforms (mechanical 1/4 period). (b) Spectrum analysis (mechanical 1 period).

Fig. 3 shows the difference in cogging torque of SPMSM with step-skew between 2-D and 3-D FEA, when the rotor electrically rotates one period. Specifically, the 24th cogging torque has a much higher magnitude (9.23 mNm) in the 3-D FEA. As previously discussed, the cogging torque of fundamental wave order still remains due to axial leakage flux. It was confirmed that the cogging torque of PMSM with step-skew is not reliable for 2-D FEA results. Therefore, in the design stage of the SPMSM applying step-skew, axial leakage flux should be considered.

B. Cogging Torque Tendency by Geometry Variables

As previously analyzed, the 24th cogging torque in the SPMSM with step-skew is caused by the leakage flux at both ends of the PMs and the leakage flux at the junction between the PMs. The magnitude of the 24th cogging torque based on 3-D FEA, which is not offset even when step-skew is applied, is expected to increase as the magnitude of 2-D FEA-based 24th cogging torque without step-skew increases. Therefore, to verify this, the tendency of the 2-D and 3-D FEA-based 24th cogging torque according to the main geometry variables that have a significant effect on the cogging torque was investigated based on the target model. Slot opening width, tooth tip thickness, and pole angle were set as geometry variables, and the 2-D and 3-D FEA results are shown in Fig. 4. As expected, the 3-D FEA-based cogging torque of the target harmonic order in the SPMSM with step-skew exhibits a similar tendency to the 2-D FEA-based cogging torque of the fundamental wave order in the SPMSM without step-skew as the geometry variables change, where the FEA was performed by varying only certain geometry variables while keeping the other geometry variables fixed in the target model. In other words, the slot opening width, tooth tip thickness, and pole angle were varied separately based on the geometry of the

Authorized licensed use limited to: Hanyang University. Downloaded on October 25,2023 at 00:35:08 UTC from IEEE Xplore. Restrictions apply.

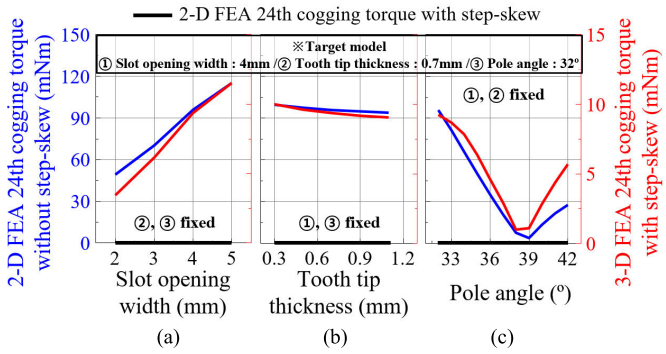

Fig. 4. 2-D and 3-D FEA-based 24th cogging torque tendency of SPMSM according to geometry variables. (a) Slot opening width. (b) Tooth tip thickness. (c) Pole angle.

TABLE II
COGGING TORQUE DATASETS USED ACCORDING TO DESIGN METHOD

Conventional method	Proposed method
1000 2-D FEA-based cogging torque with step-skew	1000 2-D FEA-based cogging torque with step-skew 1000 2-D FEA-based cogging torque without step-skew 150 3-D FEA-based cogging torque with step-skew

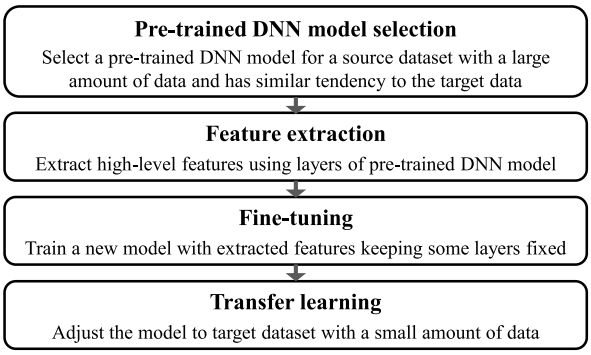

Fig. 5. Process of DNN-based transfer learning.

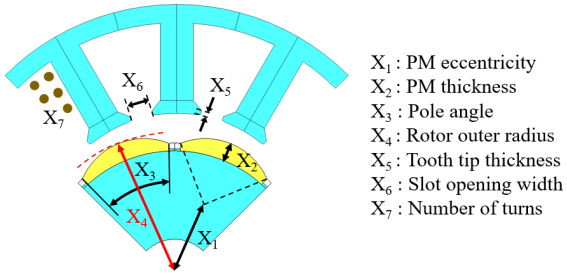

Fig. 6. Design variables.

target model. This similar tendency was used in the design method.

III. Design Method Based on Transfer Learning

In this section, the proposed design method using transfer learning to consider the axial leakage flux with low computation time for cogging torque reduction of PMSM with step-skew is described and compared with the conventional design method that does not consider the axial leakage flux. The design specifications are the same as Table I for the target model shown previously. Table II shows the datasets used according to the design method. In the proposed method, an additional small amount of 3-D FEA-based cogging torque with step-skew is required to consider the effect of the 24th cogging torque due to axial leakage flux.

A. Transfer Learning With DNN

A deep neural network (DNN) is composed of multiple layers of artificial neurons that process input data and gradually learn to recognize features within it. DNNs are capable of learning complex non-linear relationships between input and output variables, processing large amounts of data, and being trained on data from multiple sources. In addition, DNNs can reduce the number of times expensive functions need to be evaluated, providing significant savings in computational time. Therefore, DNNs are highly adopted as surrogate models for optimization [8].

Transfer learning is a deep learning technique that utilize the pre-trained domain knowledge for large amount of source dataset to predict small amount of target dataset with similar tendency to source dataset, but with a bias. Fig. 5 shows the process of DNN-based transfer learning. A pre-trained DNN model is selected based on its architecture and performance on a similar task. Subsequently, high-level features are extracted by passing the input data through the pre-trained layers of the model. From these features, a new model is trained. Finally, the general features learned from the pre-trained dataset are utilized to learn the specific features of the target task.

B. Proposed Design Process

In the proposed design process, design variables sensitive to the cogging torque were selected, as shown in Fig. 6. With these design variables, the optimal design was carried out in the same process, as shown in Fig. 7. First, the objective function and constraints are determined in the formulation stage. The objective function was defined to minimize the cogging torque, and the constraints were established based on the design specifications. Second, DNN-based surrogate models for optimization are created. To create DNN models, 1000 and 150 experimental points were extracted through the design of experiment based on optimal Latin hypercube design (OLHD), which distributes the experimental points, so that the minimum distance between the points is maximized depending on the range of design variables for optimization, as shown in Table III, and the corresponding 1000 2-D FEA-based source data and 150 3-D FEA-based target data were obtained. As previously demonstrated, the 3-D FEA-based 24th cogging torque in the PMSM with step-skew exhibits a similar tendency to the 2-D FEA-based 24th cogging torque in the PMSM without step-skew. A large amount of 2-D FEA-based data can be acquired more faster than the 3-D FEA-based data. Therefore, 1000 2-D FEA data and 150 3-D FEA data are obtained for transfer learning. In other words, for each of the 1000 experimental points, the 2-D FEA was performed under the no-load analysis condition. Then, the peak-to-peak cogging torque with step-skew and the magnitude of the 24th cogging torque without step-skew were calculated. In addition, 3-D FEA was performed under no-load analysis condition

Authorized licensed use limited to: Hanyang University. Downloaded on October 25,2023 at 00:35:08 UTC from IEEE Xplore. Restrictions apply.

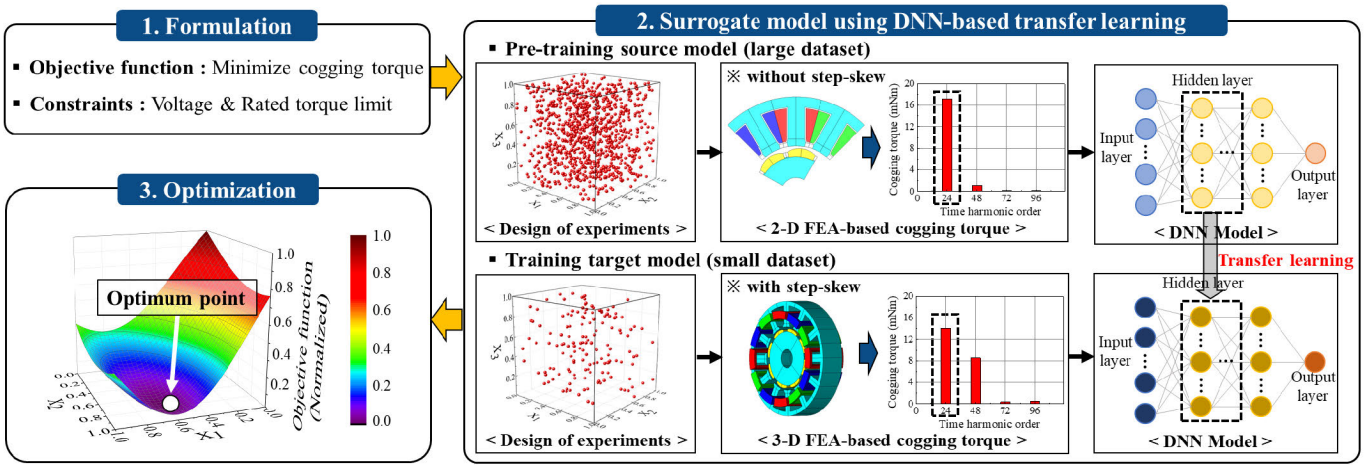

Fig. 7. Proposed transfer learning-based design process.

TABLE III
RANGE OF DESIGN VARIABLES FOR OPTIMIZATION

Parameters	Lower / Upper boundary	Unit
PM eccentricity (X_1)	0.0 / 14.0	mm
PM thickness (X_2)	2.5 / 4.0	mm
Pole angle (X_3)	32.0 / 40.0	°
Rotor outer radius (X_4)	19.35 / 25.8	mm
Tooth tip thickness (X_5)	0.5 / 2.5	mm
Slot opening width (X_6)	1.0 / 4.0	mm
Number of turns (X_7)	42 / 56	-

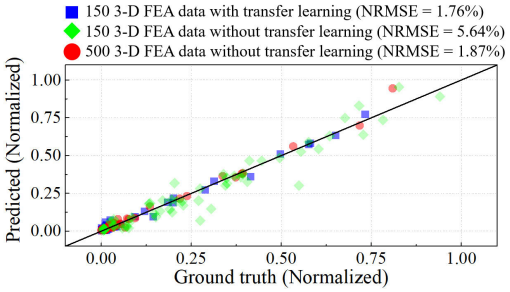

Fig. 8. Comparison of ground truth and predicted values for 24th cogging torque with step-skew depending on the number of 3-D FEA data and transfer learning.

for 150 experimental points. Then, the 24th magnitude of the cogging torque with step-skew was calculated. Similarly, to create DNN models for predicting constraints, 2-D FEA was performed under rated load condition for 1000 experimental points and line-to-line voltage and load torque were calculated. Afterward, to predict the objective function, one DNN model (DNN1) was created using 1000 2-D FEA-based peak-to-peak cogging torque data with step-skew and another DNN model (DNN2) was created using 1000 2-D FEA-based 24th cogging torque data without step-skew and 150 3-D FEA-based 24th cogging torque data with step-skew by transfer learning to consider 3-D leakage flux. Moreover, DNN models were created with 1000 2-D FEA-based line-to-line voltage and load torque data to predict the constraints, respectively. Finally, the optimization was performed using genetic algorithm (GA) to minimize the specified objective function and satisfy the constraints [9].

The optimization problem is defined as follows:

$$\begin{aligned} &\min\ T_{\text{cog}} \\ &\text{s.t. } T \geq T_{\text{rated}} \\ &\quad V_L \leq V_{L\_\max} \end{aligned} \tag{3}$$

where T_{cog} is the cogging torque, T is the load torque, T_{rated} is the rated torque (2.1 Nm), V_L is the line-to-line voltage, and $V_{L\_\max}$ is the maximum line-to-line voltage.

To minimize the objective function, only DNN1 was used in the conventional method, while both DNN1 and DNN2 were used in the proposed method. To verify the effectiveness of the proposed design method, two optimized models were derived using each method and the cogging torque performance was compared.

C. Validation and Performance of DNN Models

DNN models consist of a multi-layer perceptron structure, which is determined through hyperparameter tuning. To evaluate the model's performance on unseen data and avoid overfitting, the source data and target data were divided into training, validation, and test sets in a ratio of 8:1:1. Through hyperparameter tuning, the number of learning rate, hidden layers, and units were determined to be 5e-3, 4, and 256, respectively. The regression performance of the three DNN models predicting torque, line-to-line voltage, and peak-to-peak cogging torque is well evaluated using 100 test datasets out of 1000 2-D FEA dataset, where the normalized root mean squared error (NRMSE) is 1.24%, 1.87%, and 1.65%, respectively. In addition, the regression performance of the DNN model predicting the 24th cogging torque with step-skew varies depending on the number of 3-D FEA data and transfer learning, as shown in Fig. 8. Then, it can be seen that by using transfer learning, a DNN model with a better performance based on the same amount of 3-D FEA data can be built, and a DNN model with similar performance can be built with smaller 3-D FEA data. In fact, it is possible to perform fewer 3-D FEA that require a lot of computation time compared to 2-D FEA. Therefore, through the proposed method, it is shown that the 24th cogging torque with step-skew can be

Authorized licensed use limited to: Hanyang University. Downloaded on October 25,2023 at 00:35:08 UTC from IEEE Xplore. Restrictions apply.

TABLE IV
RESULTS OF CONVENTIONAL MODEL AND PROPOSED MODEL

Parameters	Conventional model	Proposed model
PM eccentricity (mm)	6.7	11.0
PM thickness (mm)	3.17	3.75
Pole angle (°)	32.5	39.0
Rotor outer radius (mm)	20.63	22.7
Tooth tip thickness (mm)	0.71	0.7
Slot opening width (mm)	3.98	4.0
Number of turns	52	42
2-D FEA-based peak-to-peak cogging torque with step-skew (mNm)	0.67	0.47
2-D FEA-based 24th cogging torque without step-skew (mNm)	109.0	0.81
3-D FEA-based 24th cogging torque with step-skew (mNm)	11.66	1.55

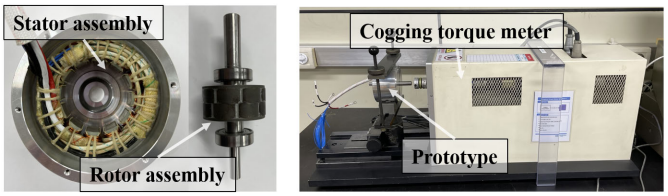

(a) (b)

Fig. 9. Fabricated prototype of the proposed model consisting of (a) stator and rotor assembly and (b) cogging torque test setup.

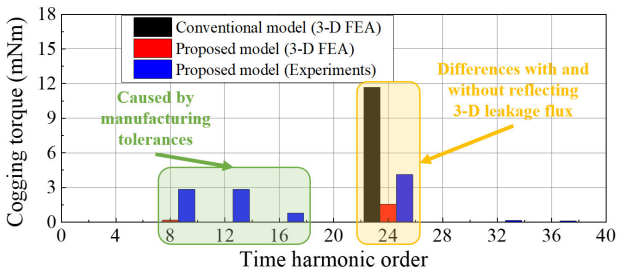

Fig. 10. Spectrum analysis comparison of 3-D FEA and experimental cogging torque with step-skew between conventional model and proposed model (mechanical 1 period).

well predicted by considering the axial leakage flux with a small amount of 3-D FEA-based 24th cogging torque data using transfer learning.

IV. DESIGN RESULTS AND EXPERIMENTAL VERIFICATION

Table IV shows the results of the conventional model and proposed model derived for each design method. The 2-D FEA-based peak-to-peak cogging torque with step-skew is similar for the conventional model and the proposed model, but the 2-D FEA-based 24th cogging torque without step-skew is more than 130 times larger for the conventional model than for the proposed model. Similarly, the 3-D FEA-based 24th cogging torque with step-skew is more than 10 times larger for the conventional model than for the proposed model.

A prototype was fabricated and tested with a cogging torque meter, as shown in Fig. 9. By measuring the cogging torque of the proposed model, it was confirmed that the 24th cogging is reduced. Except for the 8th, 12th, and 16th cogging torques caused by manufacturing tolerance [10], the 24th cogging torque is significantly reduced compared to the conventional model, as shown in Fig. 10. The error of the 24th cogging torque with step-skew between the 3-D FEA and experiments of the proposed model is caused by the assembly tolerance of the skew angle and the axial leakage flux.

V. CONCLUSION

This article proposes a computationally efficient design method for cogging torque reduction of PMSM with step-skew while considering the 3-D leakage flux. The similar tendency of 2-D FEA-based cogging torque of fundamental wave order without step-skew and 3-D FEA-based cogging torque of fundamental wave order with step-skew according to the design variables was used to utilize transfer learning. Through the proposed design method, a surrogate model with higher accuracy can be created even with a small amount of 3-D FEA-based data. Accordingly, it was confirmed that the PMSM designed by the proposed method has better cogging torque performance than the PMSM designed by the conventional method that does not consider 3-D leakage flux. Furthermore, a prototype was fabricated and verified by experimental evaluation that a superior model is designed by the proposed method than the conventional method. Consequently, the proposed design method can be applied to the design of cogging torque reduction by considering 3-D leakage flux with low computation time.

ACKNOWLEDGMENT

This work was supported by the National Research Foundation of Korea (NRF) grant funded by the Korea Government [Ministry of Science and ICT (MSIT)] (No. RS-2023-00207865).

REFERENCES

[1] J. R. Hendershot and T. J. E. Miller, *Design of Brushless Permanent Magnet Machines*, vol. 2, 2nd ed. Oxford, U.K.: Clarendon, 2010, pp. 111–115.
[2] S.-M. Hwang, J.-B. Eom, Y.-H. Jung, D.-W. Lee, and B.-S. Kang, "Various design techniques to reduce cogging torque by controlling energy variation in permanent magnet motors," *IEEE Trans. Magn.*, vol. 37, no. 4, pp. 2806–2809, Jul. 2001.
[3] Z. Q. Zhu and D. Howe, "Influence of design parameters on cogging torque in permanent magnet machines," *IEEE Trans. Energy Convers.*, vol. 15, no. 4, pp. 407–412, Dec. 2000.
[4] N. Bianchi and S. Bolognani, "Design techniques for reducing the cogging torque in surface-mounted PM motors," *IEEE Trans. Ind. Appl.*, vol. 38, no. 5, pp. 1259–1265, Sep. 2002.
[5] W. Fei and P. Luk, "A new technique of cogging torque suppression in direct-drive permanent-magnet brushless machines," *IEEE Trans. Ind. Appl.*, vol. 46, no. 4, pp. 1332–1340, Jul. 2010.
[6] S.-M. Hwang, J.-B. Eom, G.-B. Hwang, W.-B. Jeong, and Y.-H. Jung, "Cogging torque and acoustic noise reduction in permanent magnet motors by teeth pairing," *IEEE Trans. Magn.*, vol. 36, no. 5, pp. 3144–3146, Sep. 2000.
[7] D. Wang, X. Wang, and S.-Y. Jung, "Reduction on cogging torque in flux-switching permanent magnet machine by teeth notching schemes," *IEEE Trans. Magn.*, vol. 48, no. 11, pp. 4228–4231, Nov. 2012.
[8] S.-H. Park, J.-W. Chin, K.-S. Cha, and M.-S. Lim, "Deep transfer learning-based sizing method of permanent magnet synchronous motors considering axial leakage flux," *IEEE Trans. Magn.*, vol. 58, no. 9, pp. 1–5, Sep. 2022.
[9] B. A. Skinner, G. T. Parks, and P. R. Palmer, "Comparison of submarine drive topologies using multiobjective genetic algorithms," *IEEE Trans. Veh. Technol.*, vol. 58, no. 1, pp. 57–68, Jan. 2009.
[10] J. Ou, Y. Liu, R. Qu, and M. Doppelbauer, "Experimental and theoretical research on cogging torque of PM synchronous motors considering manufacturing tolerances," *IEEE Trans. Ind. Electron.*, vol. 65, no. 5, pp. 3772–3783, May 2018.

Authorized licensed use limited to: Hanyang University. Downloaded on October 25,2023 at 00:35:08 UTC from IEEE Xplore. Restrictions apply.